

## Coral-like $\text{Ni}_x\text{Co}_{1-x}\text{Se}_2$ for Na-ion battery with ultralong cycle life and ultrahigh rate capability

*Yanyan He,<sup>a,d</sup> Ming Luo,<sup>a</sup> Caifu Dong,<sup>a</sup> Xuyang Ding,<sup>a</sup> Chaochuang Yin,<sup>c</sup> Anmin Nie,<sup>e</sup>*

*Yanan Chen,<sup>\*c</sup> Yitai Qian<sup>a</sup> and Liqiang Xu<sup>\*a,b</sup>*

<sup>a</sup> Key Laboratory of Colloid and Interface Chemistry, Ministry of Education, School of Chemistry and Chemical Engineering, Shandong University, Jinan, 250100, China

<sup>b</sup> Shenzhen Research Institute of Shandong University, Rm A301, Virtural University Park, Nanshan, Shenzhen 518057, Guangdong Province, China

\*E-mail: [xulq@sdu.edu.cn](mailto:xulq@sdu.edu.cn)

<sup>c</sup> School of Life Sciences, Tsinghua University, Beijing, 100084, China

<sup>d</sup> Engineering, Qilu University of Technology (Shandong Academy of Sciences), Jinan 250353, People's Republic of China.E-mail: [yananchen@tsinghua.edu.cn](mailto:yananchen@tsinghua.edu.cn)

<sup>e</sup> State Key Lab of Metastable Materials Science and Technology, Yanshan University, Qinhuangdao, 066004, China

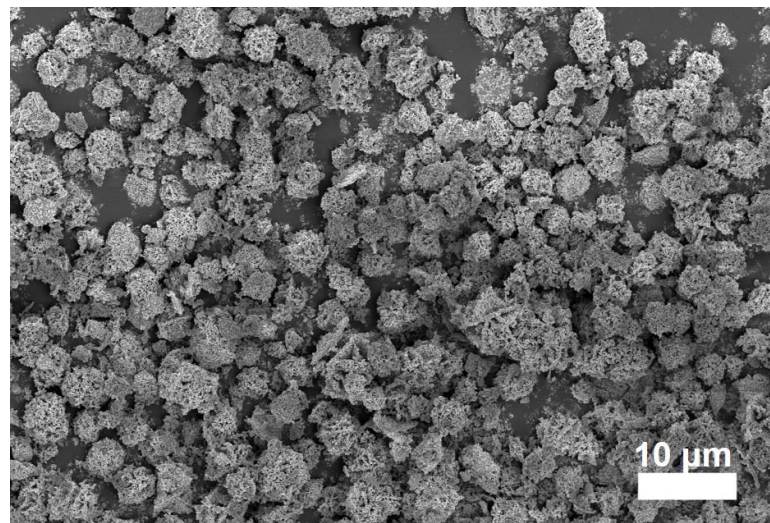


**Fig. S1** Large area SEM image of  $\text{Ni}_{0.47}\text{Co}_{0.53}\text{Se}_2$  micro-nanosphere.



**Fig. S2** Energy dispersive spectrometer (EDS) analysis of  $\text{Ni}_{0.47}\text{Co}_{0.53}\text{Se}_2$  micro-nanosphere.

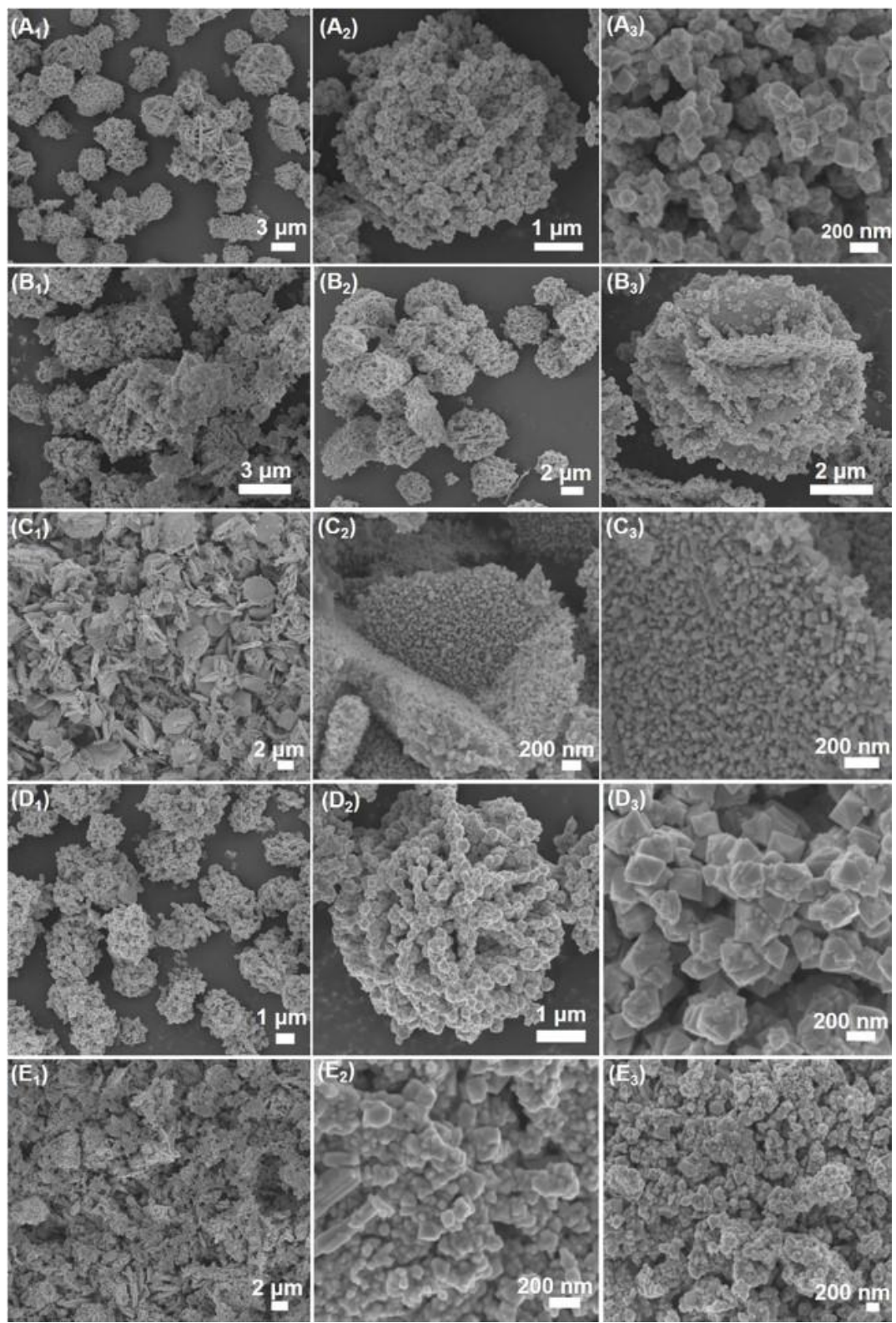


**Fig. S3** SEM images of  $\text{Ni}_x\text{Co}_{1-x}\text{Se}_2$  with different ratios of Ni and Co. (A<sub>1</sub>-A<sub>3</sub>)  $\text{Ni}_{0.72}\text{Co}_{0.28}\text{Se}_2$ , (B<sub>1</sub>-B<sub>3</sub>)  $\text{Ni}_{0.67}\text{Co}_{0.33}\text{Se}_2$ , (C<sub>1</sub>-C<sub>3</sub>)  $\text{Ni}_{0.31}\text{Co}_{0.69}\text{Se}_2$ , (D<sub>1</sub>-D<sub>3</sub>)  $\text{Ni}_{0.79}\text{Co}_{0.21}\text{Se}_2$  and (E<sub>1</sub>-E<sub>3</sub>)  $\text{Ni}_{0.17}\text{Co}_{0.83}\text{Se}_2$ .

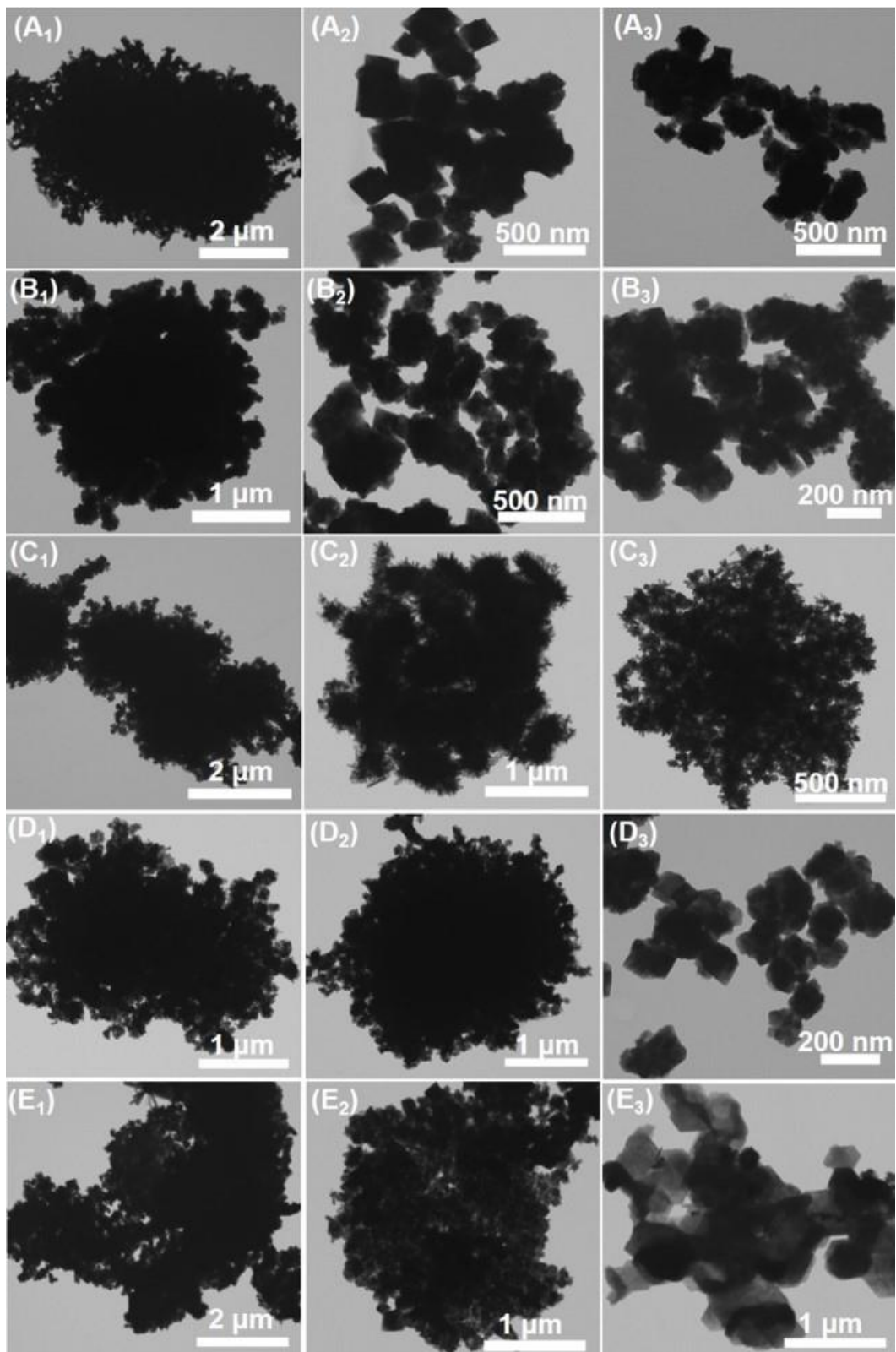


**Fig. S4** TEM images of  $\text{Ni}_x\text{Co}_{1-x}\text{Se}_2$  with different ratios of Ni and Co. (A<sub>1</sub>-A<sub>3</sub>)  $\text{Ni}_{0.72}\text{Co}_{0.28}\text{Se}_2$ , (B<sub>1</sub>-B<sub>3</sub>)  $\text{Ni}_{0.67}\text{Co}_{0.33}\text{Se}_2$ , (C<sub>1</sub>-C<sub>3</sub>)  $\text{Ni}_{0.31}\text{Co}_{0.69}\text{Se}_2$ , (D<sub>1</sub>-D<sub>3</sub>)  $\text{Ni}_{0.79}\text{Co}_{0.21}\text{Se}_2$  and (E<sub>1</sub>-E<sub>3</sub>)  $\text{Ni}_{0.17}\text{Co}_{0.83}\text{Se}_2$ .

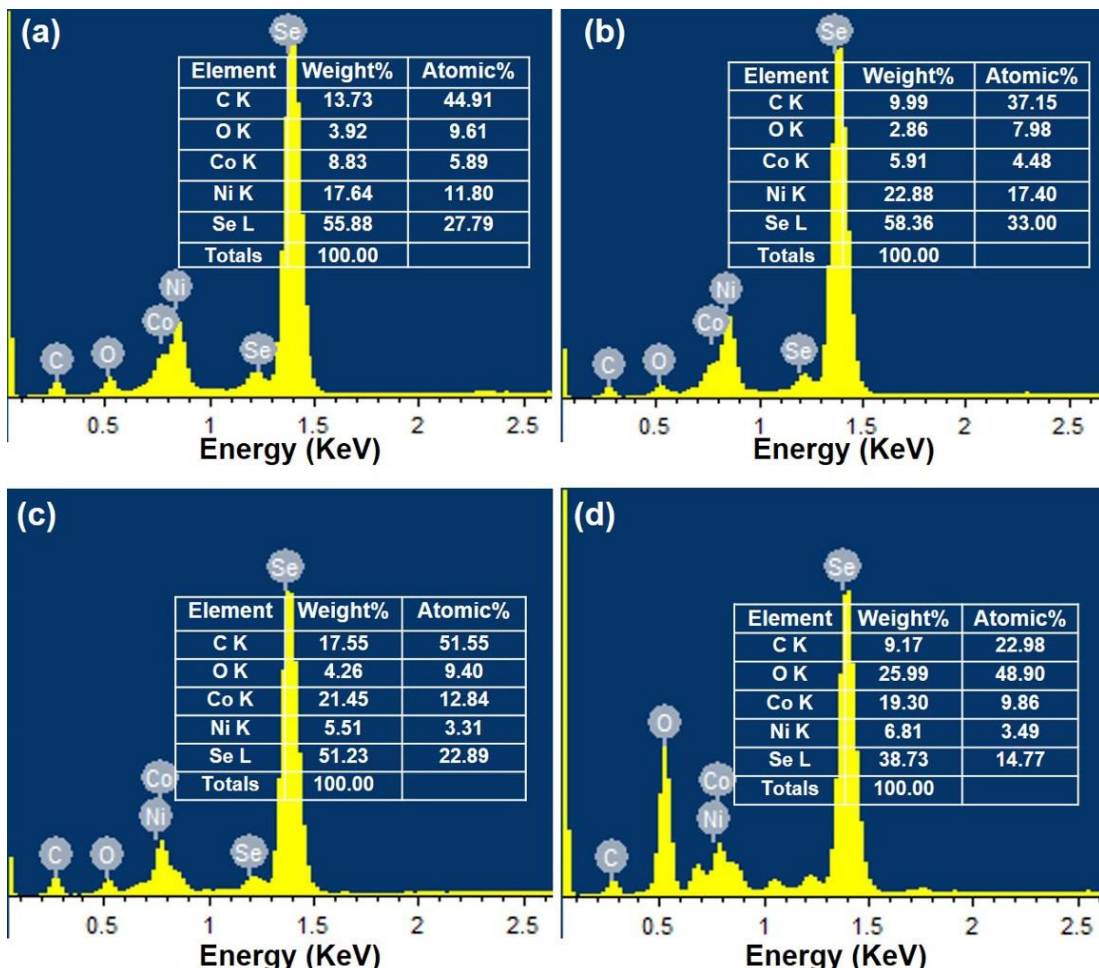


**Fig. S5** Energy dispersive spectrometer (EDS) analysis of (a)  $\text{Ni}_{0.67}\text{Co}_{0.33}\text{Se}_2$ , (b)  $\text{Ni}_{0.79}\text{Co}_{0.21}\text{Se}_2$ , (c)  $\text{Ni}_{0.17}\text{Co}_{0.83}\text{Se}_2$  and (d)  $\text{Ni}_{0.23}\text{Co}_{0.77}\text{Se}_2$ .

**Table S1.** The ICP-OES analysis results of  $\text{Ni}_x\text{Co}_{1-x}\text{Se}_2$  with different ratios of Ni/Co.

Samples	Contents of Co (mg/L)	Contents of Ni (mg/L)
$\text{Ni}_{0.17}\text{Co}_{0.83}\text{Se}_2$	4.071	0.859
$\text{Ni}_{0.23}\text{Co}_{0.77}\text{Se}_2$	4.087	1.212
$\text{Ni}_{0.31}\text{Co}_{0.69}\text{Se}_2$	6.125	2.727
$\text{Ni}_{0.47}\text{Co}_{0.53}\text{Se}_2$	4.915	4.345
$\text{Ni}_{0.72}\text{Co}_{0.28}\text{Se}_2$	2.063	5.187
$\text{Ni}_{0.79}\text{Co}_{0.21}\text{Se}_2$	1.303	4.761

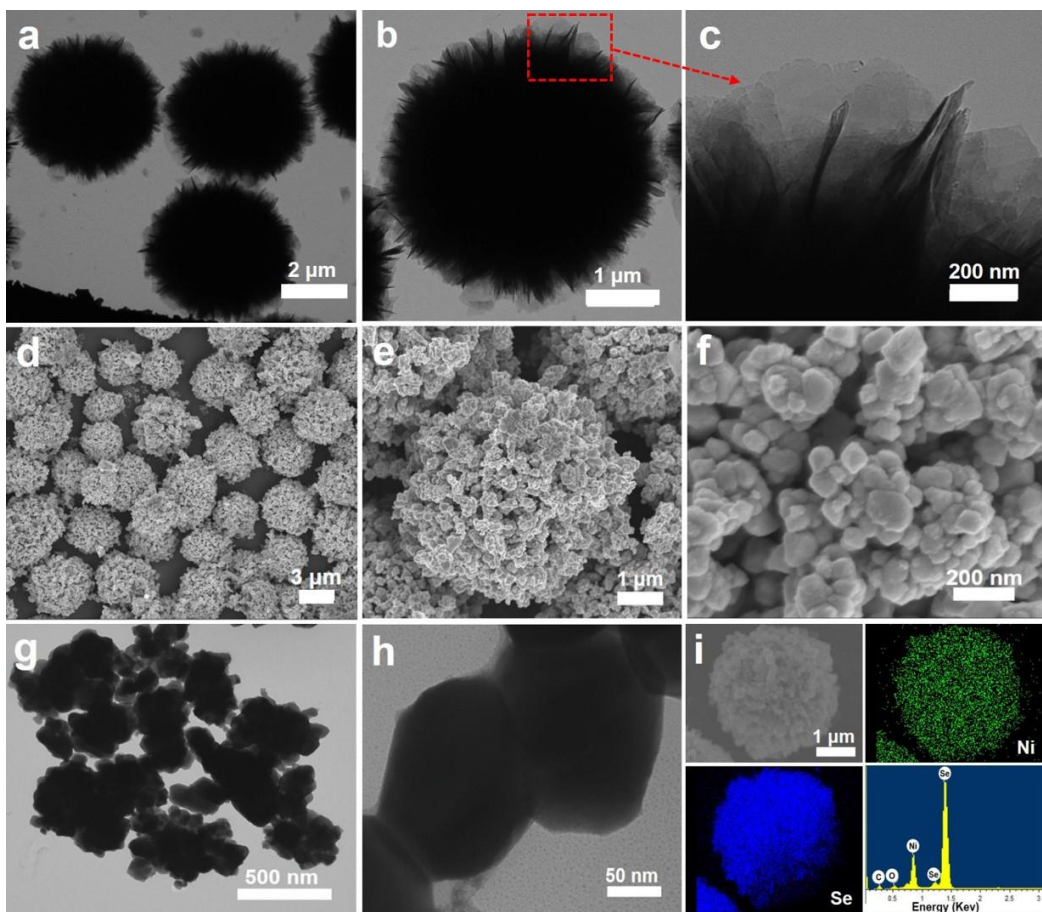


**Fig. S6** (a-c) TEM images of Ni-Co based precursor. (d-f) SEM images, (g, h) TEM image and (i) Elemental mappings and EDS spectrum of hierarchical NiSe<sub>2</sub> micro-nanospheres.

Element	Weight%	Atomic%
C K	12.12	42.70
O K	2.52	6.67
Ni K	26.28	18.95
Se L	59.08	31.68
<b>Totals</b>	<b>100.00</b>	

**Fig. S7** Energy dispersive spectrometer (EDS) analysis of NiSe<sub>2</sub> micro-nanosphere.

Fig. S6 (a-c) show the TEM images of Ni based precursor, it presents micro-nanosphere morphology with size of 3~4  $\mu\text{m}$ , which is composed of thin nanosheet structures. The SEM images (Fig. S6d-f) indicate the micro-nanostructure still preserves its integrated nature (3~4  $\mu\text{m}$ ), however, the nanosheets in the precursor have transformed to nanoparticles after selenization process, and the size of nanoparticles are ~100 nm. Fig. S6g and Fig. S6h shows the TEM images of the nanoparticles dropped from the micro-nanosphere, which further deliver the size of nanoparticles are ~100 nm. In addition, the Elemental mapping (Fig. S6i) indicates the coexistence of Ni and Se in the micro-nanosphere and the EDS analysis (Fig. S7) presents a Ni/Se mole ratio of ~1:2 for hierarchical NiSe<sub>2</sub> micro-nanosphere.

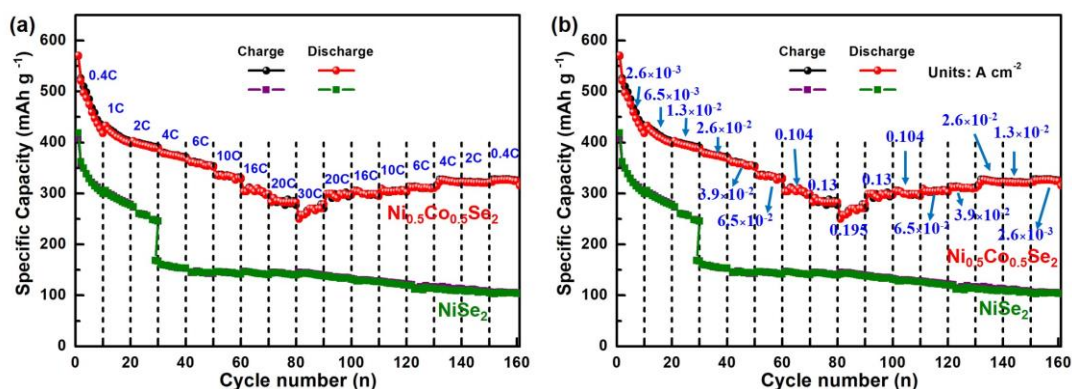


**Fig. S8** Rate performances of Ni<sub>0.47</sub>Co<sub>0.53</sub>Se<sub>2</sub> and NiSe<sub>2</sub> materials. The units of the current densities are (a) C-rate and (b) A cm<sup>-2</sup>, respectively.

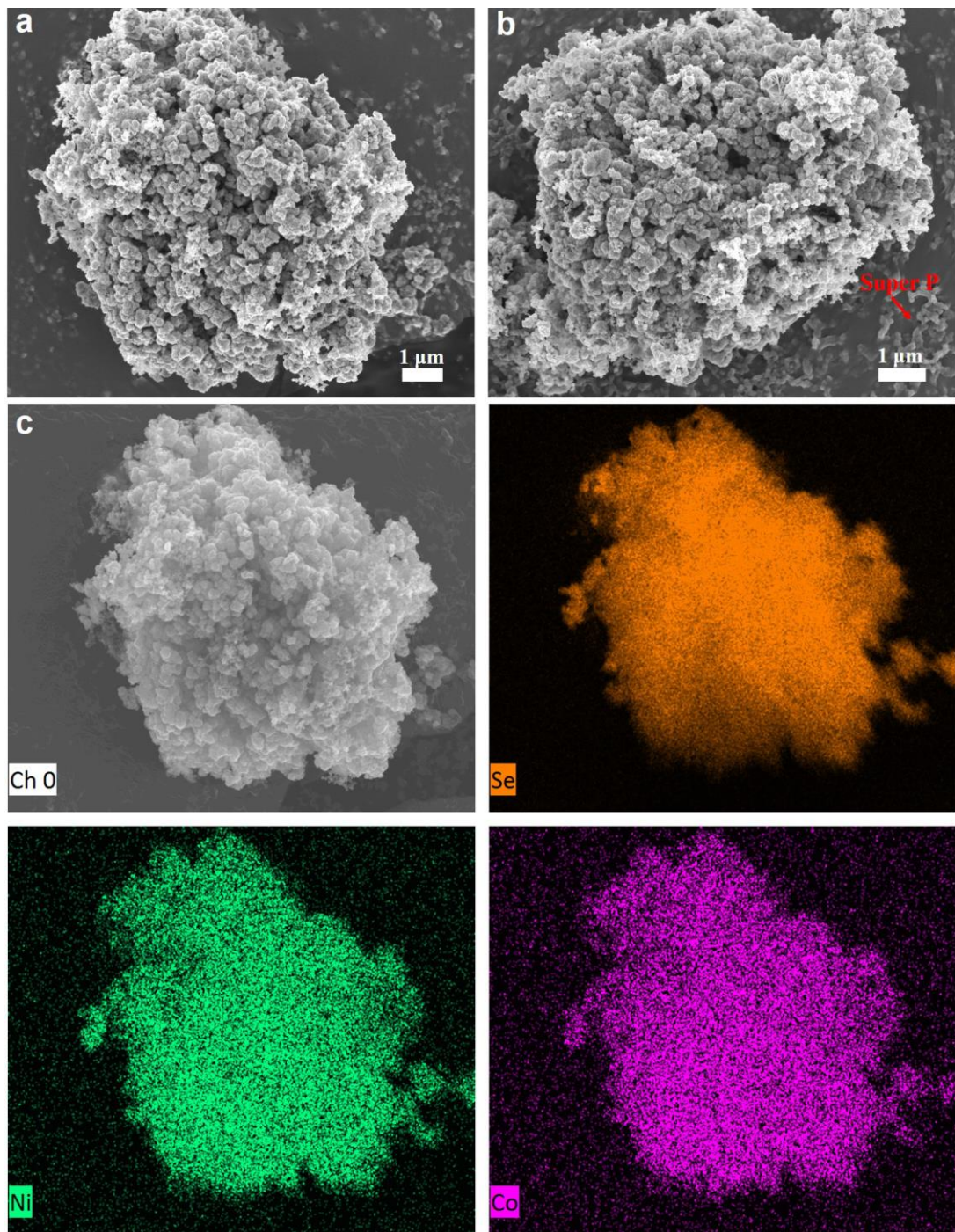


**Fig. S9** (a, b) SEM images and (c) elemental mapping of  $\text{Ni}_{0.47}\text{Co}_{0.53}\text{Se}_2$  material after 50 cycles at a current density of  $1 \text{ A g}^{-1}$ .

**Table S2.** The comparison of electrochemical performances between the hierarchical  $\text{Ni}_{0.47}\text{Co}_{0.53}\text{Se}_2$  micro-nanosphere electrodes with the reported nickel/cobalt selenide related electrodes when applied as anode materials for SIBs.

<b>Materials</b>		<b>Specific capacity, mAh g<sup>-1</sup>/Cycle numbers, (Current density, A g<sup>-1</sup>)</b>	<b>Specific capacity, mAh g<sup>-1</sup>/High current density, A g<sup>-1</sup></b>	<b>Ref.</b>
Graphene-wrapped $\text{NiSe}_2/\text{C}$ nanofiber		468/100 <sup>th</sup> , (0.2)	269/2 243/3	[1]
$\text{NiSe}_2/\text{rGO}$ hybrid		346/1000 <sup>th</sup> , (1)	347/2 318/5	[2]
$\text{NiSe}_2$ nanoctahedra		313/4000 <sup>th</sup> , (5)	< 200/15 175/20	[3]
Square nanoplates	$\text{NiSe}_2$	311/100 <sup>th</sup> , (1)	249/5 213/10	[4]
$\text{MoSe}_2\text{-NiSe-C}$ composite		386/80 <sup>th</sup> , (0.5)		[5]
microsphere			301/3	
$\text{Ni}_{0.85}\text{Se/C}$ hollow nanowires		390/100 <sup>th</sup> , (0.83)	219/2.1 172/4.2	[6]
core-shell $\text{NiSe/C}$ nanospheres		280/50 <sup>th</sup> , (0.1)	235/0.2 186/0.5	[7]
Hollow Selenide Microspheres	Cobalt	~425/40 <sup>th</sup> , (0.5)	466/0.9	[8]
$\text{CoSe}_x\text{-rGO}$ Composite		~336/50 <sup>th</sup> , (0.3)	357/1	[9]
Yolk–Shell-Structured $\text{CoSe/C}$		536/50 <sup>th</sup> , (0.5)	361.9/16	[10]
Ultrathin $\text{Co}_9\text{Se}_8/\text{rGO}$ Hybrid Nanosheets		406/100 <sup>th</sup> , (0.05)	295/5	[11]
$\text{CoSe}_2/(\text{NiCo})\text{Se}_2$ hollow nanocubes		497/80 <sup>th</sup> , (0.2)	456/5	[12]
<b>Our work</b>			360.2/5	
<b>(hierarchical <math>\text{Ni}_{0.47}\text{Co}_{0.53}\text{Se}_2</math> micro-nanosphere)</b>		321/2000 <sup>th</sup> , (2)	324.5/10 277/15	

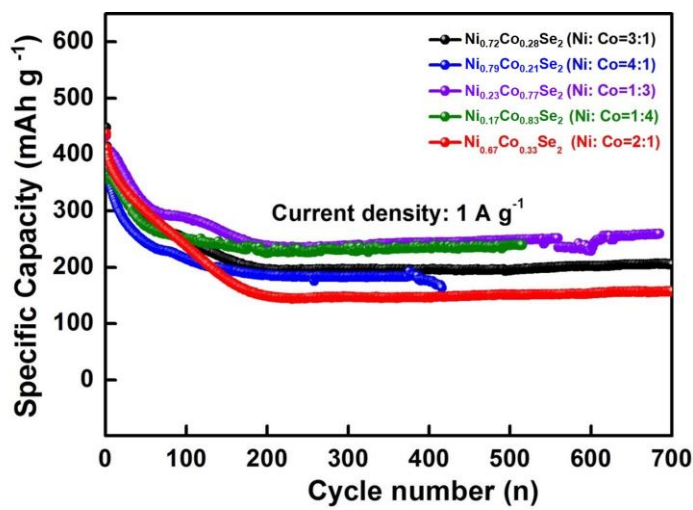


**Fig. S10** The cycle performances of  $\text{Ni}_x\text{Co}_{1-x}\text{Se}_2$  with different ratios of Ni/Co at current density of  $1 \text{ A g}^{-1}$  in ether-based electrolyte (1M  $\text{CF}_3\text{NaSO}_3$  in DEGDME).

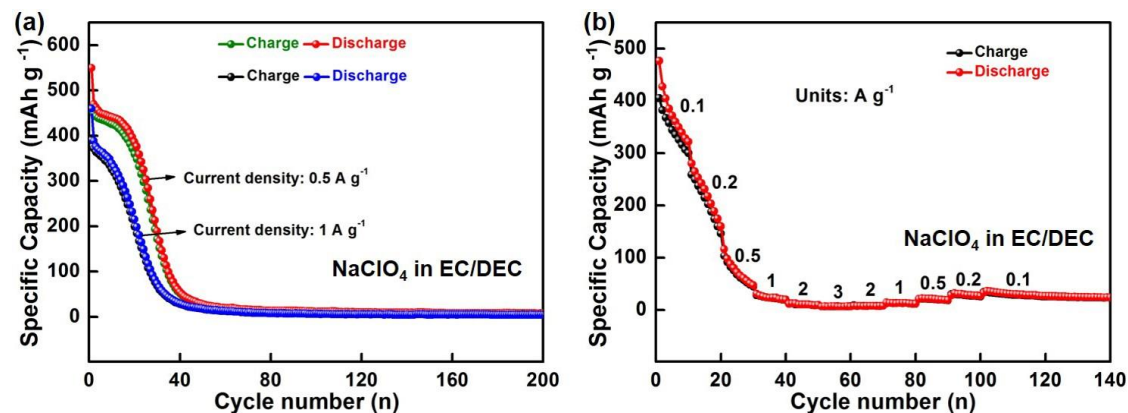


**Fig. S11** (a) Cycle performances at current densities of 0.5 and  $1 \text{ A g}^{-1}$ , and (b) rate performance of hierarchical  $\text{Ni}_{0.47}\text{Co}_{0.53}\text{Se}_2$  micro-nanospheres electrode in carbonate-based electrolyte (1M  $\text{NaClO}_4$  in EC/DEC).

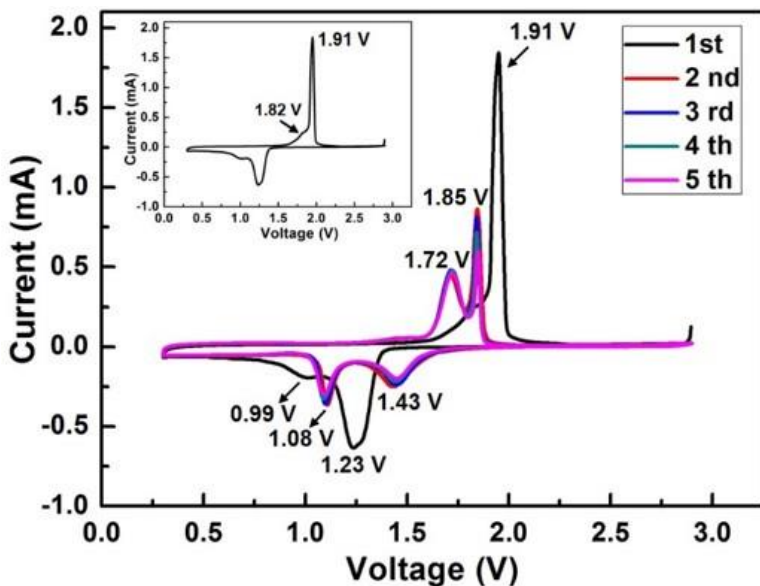


**Fig. S12** CV curves of the hierarchical NiSe<sub>2</sub> micro-nanosphere electrode with scan rate of 0.1 mV s<sup>-1</sup> for SIBs. (The insert one is the first cycle curve).

During the first discharge process, the reduction peaks located at 1.23 V and 0.99 V, might correspond to the insertion of Na<sup>+</sup> into NiSe<sub>2</sub> and resulting the conversion reaction to form Na<sub>2</sub>Se and metallic Ni nanocrystals (NiSe<sub>2</sub> + 4Na<sup>+</sup> + 4e<sup>-</sup> → Ni + 2Na<sub>2</sub>Se)<sup>1,2,7</sup>. During the first charge process, the weak oxidation peak located at 1.83 V and the sharp oxidation peaks located at 1.91 V might be attributed to the deintercalation of Na<sup>+</sup> and the recovery of NiSe<sub>2</sub> from Na<sub>2</sub>Se and metallic Ni nanocrystals (Ni + 2Na<sub>2</sub>Se → NiSe<sub>2</sub>)<sup>1,2,7</sup>. In the second cycle, the position of reduction peaks shifted to higher potentials, which might be related to the formation of ultrafine nanocrystals during the first cycle.

## Reference

1. J. S. Cho, S. Y. Lee and Y. C. Kang, *Sci. Rep.*, 2016, **6**, 23338-22510.
2. X. Ou, J. Li, F. H. Zheng, P. Wu, Q. C. Pan, X. H. Xiong, C. H. Yang and M. L. Liu, *J. Power. Sources*, 2017, **343**, 483-491.
3. S. H. Zhu, Q. D. Li, Q. L. Wei, R. M. Sun, X. Q. Liu, Q. Y. An and L. Q. Mai, *ACS Appl. Mater. Interfaces*, 2017, **9**, 311-316.
4. H. S. Fan, H. Yu, X. L. Wu, Y. Zhang, Z. Z. Luo, H. W. Wang, Y. Y. Guo, S. Madhavi and Q. Y. Yan, *ACS Appl. Mater. Interfaces*, 2016, **8**, 25261-25267.
5. J. S. Park and Y. C. Kang, *J. Mater. Chem. A*, 2017, **5**, 8616-8623.

6. X. M. Yang, J. L. Zhang, Z. G. Wang, H. K. Wang, C. Y. Zhi, D. Y. W. Yu and A. L. Rogach, *Small*, 2018, **14**, 1702669.
7. Z. A. Zhang, X. D. Shi and X. Yang, *Electrochimi. Acta*, 2016, **208**, 238-243.
8. Y. N. Ko, S. H. Choi and Y. C. Kang, *ACS Appl. Mater. Interfaces*, 2016, **8**, 6449-6456.
9. G. D. Park and Y. C. Kang, *Chem. Eur. J.*, 2016, **22**, 4140-4146.
10. Y. F. Zhang, A. Q. Pan, L. Ding, Z. L. Zhou, Y. P. Wang, S. Y. Niu, S. Q. Liang and G. Z. Cao, *ACS Appl. Mater. Interfaces*, 2017, **9**, 3624-3633.
11. X. F. Wang, D. Z. Kong, Z. X. Huang, Y. Wang and H. Y. Yang, *Small*, 2017, **13**, 1603980.
12. S. K. Park, J. K. Kim, and Y. C. Kang, *J. Mater. Chem. A*, 2017, **5**, 18823-18830.